



# Space weather impact on radio communication and navigation

Mamoru Ishii<sup>a,\*</sup>, Jens Berdermann<sup>b</sup>, Biagio Forte<sup>c</sup>, Mike Hapgood<sup>d</sup>, Mario M. Bisi<sup>d</sup>,  
Vincenzo Romano<sup>e</sup>

<sup>a</sup> National Institute of Information and Communications Research Laboratory, Nukui-Kita, Kogane, Tokyo, Japan

<sup>b</sup> DLR Institute for Solar-Terrestrial Physics, Neustrelitz, Germany

<sup>c</sup> Department of Electronic and Electrical Engineering, University of Bath, BA2 7AY Bath, UK

<sup>d</sup> RAL Space, United Kingdom Research and Innovation – Science & Technology Facilities Council – Rutherford Appleton Laboratory, Harwell Campus, Oxfordshire OX11 0QX, UK

<sup>e</sup> Istituto Nazionale di Geofisica e Vulcanologia: Roma, Lazio, Italy

Received 11 August 2023; received in revised form 21 January 2024; accepted 22 January 2024

## Abstract

It is well known that space weather can cause significant disruptions to modern communications and navigation systems, leading to increased safety risks, economic losses, and reduced quality of life. Operators of critical infrastructures (both national and international) are also increasingly aware that extreme space-weather events can have severe impacts on their systems. For example, strong ionospheric disturbances can degrade, and sometimes deny access to satellite positioning, navigation, and timing services, central to the operation of many infrastructures. The mitigation of the effects of space weather on technical systems on the ground and in space, and the development of possible protective measures, are therefore of essential importance. We discuss how space weather drives a wide variety of ionospheric phenomena that can disrupt communications and navigation systems and how scientific understanding can help us to mitigate those effects. We also provide recommendations on further research and collaboration with industrial and governmental partners, which are essential for the development and operation of space weather services.

© 2024 COSPAR. Published by Elsevier B.V. This is an open access article under the CC BY license (<http://creativecommons.org/licenses/by/4.0/>).

**Keywords:** Radio communication; Navigation; Satellite positioning; Broadcast; Ionosphere; Radio propagation

*Table of Acronyms/abbreviations:* AGW, Atmospheric Gravity Wave; ARAIM, Advanced Receiver Autonomous Integrity Monitoring; CME, Coronal Mass Ejection; EGNOS, European Geostationary Navigation Overlay Service; EPB, Equatorial Plasma Bubble; Es, Sporadic E region; EUV, Extreme UltraViolet; GAGAN, The GPS-aided GEO augmented navigation; GBAS, Ground-Based Augmentation System; GICs, Geomagnetically Induced Currents; GNSS, Global Navigation Satellite Systems; HF, High Frequency; HSS, High Speed Stream; ILS LOC, Instrument Landing System Localiser; LF, Low Frequency; LSTID, Large Scale Traveling Ionospheric Disturbance; MF, Medium Frequency; MSAS, MTSAT Satellite-based Augmentation System; MSTID, Medium Scale Traveling Ionospheric Disturbance; NavIC, Indian Regional Navigation Satellite System; PCA, Polar Cap Absorption; PPP, Precise Point Positioning; QZSS, Quasi-Zenith Satellite System; R2O2R, Research to Operation and Operation to Research; RAIM, Receiver Autonomous Integrity Monitoring; REP, Relativistic Electron Precipitation; SATCOM, Satellite Communication; SBAS, Satellite-based augmentation systems; SEP, Solar Energetic Particle; SRB, Solar Radio Burst; SWF, Short Wave Fadeout; SWx, Space Weather; TEC, Total Electron Content; TID, Traveling Ionospheric Disturbance; VDB, VHF Data Broadcast; VHF, Very High Frequency; VHF COM, VHF Communications; VLF, Very Low Frequency; VOR, VHF Omnidirectional Range station; WAAS, Wide Area Augmentation System

\* Corresponding author.

E-mail address: [mishii@nict.go.jp](mailto:mishii@nict.go.jp) (M. Ishii).

<https://doi.org/10.1016/j.asr.2024.01.043>

0273-1177/© 2024 COSPAR. Published by Elsevier B.V.

This is an open access article under the CC BY license (<http://creativecommons.org/licenses/by/4.0/>).

## 1. Introduction

Solar flares, solar energetic particles (SEPs) and coronal mass ejections (CMEs) can cause ionospheric disturbances affecting HF, VHF, and L-band signals used for radio communication and satellite-based positioning [Berdermann et al., 2018; John et al., 2021; Forte et al., in press]. In addition, solar radio bursts can emit noise in a wide range of frequencies affecting radio signals used in many critical infrastructures and services, e.g., global navigation satellite systems (GNSS), communication and radar systems [Sato et al., 2019b, 2019a]. Other more regional ionospheric phenomena that have an impact on satellite radio signals include sporadic E-layer (Es), equatorial plasma bubbles (EPBs), plasma patches, auroral precipitation and polar cap absorption.

EPBs are large-scale structures characterised by depleted electron density, with small scale ionospheric irregularities developing at their edges, caused by Rayleigh-Taylor instabilities due to the plasma flow inversion of the equatorial ionosphere at sunset times. Small-scale irregularities connected with EPBs impact the radio signal propagation and can lead to amplitude- or/and phase-scintillation at the GNSS receiver (Cesaroni et al., 2021; Hlubek et al., 2014; Kriegel et al., 2017; Berdermann and Sato, 2020). Es layers are thin dense layers of ionisation that can reflect VHF radio waves and thus can sometimes lead to VHF propagation beyond the line-of-sight. Such extraordinary propagation can interfere with VHF communication in other areas, beyond that served by the original transmission. These space weather (SWx) manifestations impact on radio signals not only during severe space weather events, because they occur much more often than satellite anomalies or geomagnetically induced currents (GICs). In this paper, we categorise space weather phenomena with potential impacts on satellite telecommunications and navigation. Furthermore, we will provide recommendations for development of forecasting services, for the maintenance and development of current and future observation capabilities, for the continuing exchange and archiving of relevant data, and for the vital role of dialogue with other scientific and engineering communities affected by space weather.

## 2. Space weather impact on radio propagation

In view of the ever-increasing demands on accuracy, reliability, availability and safety of modern radio systems in telecommunications and navigation, the necessity of establishing ionospheric information and data services in connection with space weather services is beyond question. Sensitive, low-power radio communication and navigation systems can be limited in their operational reliability or accuracy by space weather effects including anomalous reflection, refraction, delay, diffraction, and absorption of radio waves propagating through the ionosphere or directly by interference from solar radio bursts. In the field

of navigation systems, this applies both to single-frequency systems used in numerous applications today as well as to dual- and multi-frequency systems, in which amplitude/phase scintillations and other turbulent ionospheric effects lead to considerable signal disruption, hence impairing the advantages associated with the use of multiple frequencies.

The description of each phenomenon is based on Kusano (2023). More detailed discussion was shown in Tsagouri et al., 2023a, 2023b.

### (1) Short Wave Fadeout (SWF).

The Short Wave Fadeout (SWF) is a phenomenon in which a sudden increase in the intensity of X-rays during a solar flare causes a sudden increase in the electron density in the D region. This is the lowest region of the ionosphere, and is located at altitudes where the atmospheric absorption of X-rays is greatest. The enhanced electron density then results in the absorption of high-frequency (HF, 3–30 MHz) radio waves (also known as “short waves”), due to collisions between electrons and the surrounding neutral atmospheric particles. This phenomenon is also called the Dellinger phenomenon (Dellinger, 1937). The higher the electron density in the D-region, the greater the amount of absorption, and the lower the frequency of radio waves, the greater the effect (Fig. 1(b)). HF waves are usually reflected in the F region of the ionosphere, thus propagating over long spatial distances. However, when a SWF occurs and the total amount of absorption in the propagation path of the D region becomes larger than the transmission strength of the radio wave, a communication blackout occurs. The duration of an SWF depends on the duration of the X-ray emission associated with the solar flare, and ranges from several minutes to several 10 s of minutes. SWF can also lead to an attenuation of radio waves at VHF frequencies (30–300 MHz), but not a blackout. However, at much lower frequencies (below 300 kHz) the enhanced D-region electron density has very different impacts on radio propagation. In the low frequency (LF) band (30–300 kHz) radio waves can reflect off the bottom of the enhanced D-region providing a shorter path (compared to E or F-region reflections) for propagation of a “skywave” that can interfere with the “ground wave” radio signal that propagates along the surface of the Earth. The skywave signal arrives at a receiver after the ground wave signal with a delay between 35 and 1000 microseconds (US Coast Guard, 1992), with shorter, more troublesome, delays occurring if there is reflection from the D-region. This “early arrival” was an issue for the LF navigation systems, such as Decca, used prior to the widespread use of GNSS (Schrijver et al., 2015); its potential impact on modern LF systems such as enhanced-Loran is unclear. Whilst these modern systems aim to provide better separation of the ground-wave and skywave components of received signals, the development of separation techniques is still a subject of ongoing work (e.g. see Zhang et al., 2019; Zhao et al., 2022). At VLF frequencies (3–30 kHz) the gap between the ionosphere and the surface of the Earth acts as a natural waveguide, allowing VLF signals to prop-

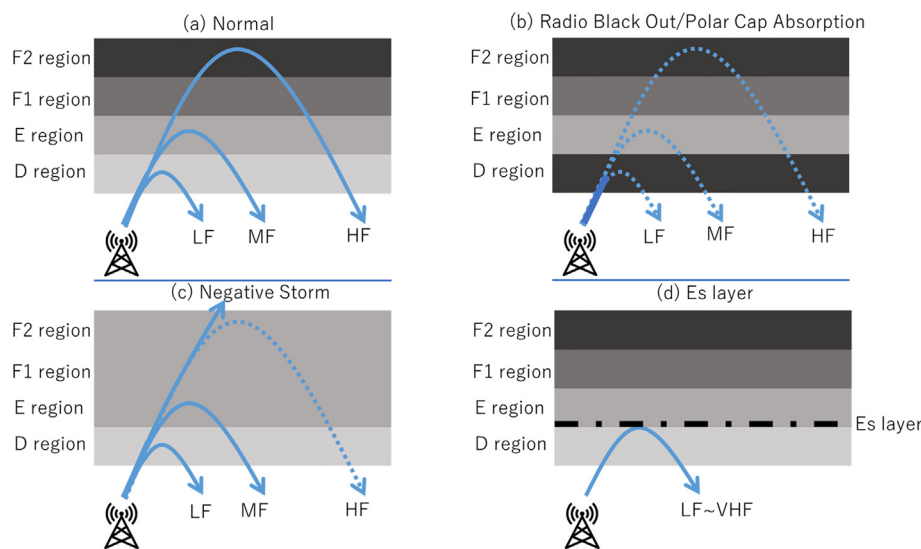


Fig. 1. Radio propagation (a) normal (b) radio black out (c) negative ionospheric storm, and (d) Es layer.

agate globally. Thus, VLF provides a means for secure global transmission of low-bandwidth radio signals, a property used for Morse code signals in the early days of radio and used today for timing signals, military communications, and scientific studies. For example, when the D-region is enhanced the waveguide narrows, leading to changes in signal phase and amplitude that can be used to detect the occurrence and intensity of solar flares (George et al., 2019).

SWF can also arise during relativistic electron precipitation (REP) events. These arise when some of the high-energy (MeV) electrons in the radiation belts are scattered to paths close to the direction of the magnetic field (Grach et al., 2022). They will then precipitate into the Earth's atmosphere rather than being magnetically mirrored above the atmosphere. Their relativistic energies lead them to deposit their energy, and create ionisation, in the D-region (Demirkol et al., 1999). A REP event over northern Europe in December 1983 caused significant disruption to the fishing industry, which then relied on LF navigation systems to avoid trawling over shipwrecks and the consequent risk of damage to equipment and risk to life arising from that damage (Fishing News, 1983).

#### (2) Solar Radio burst (SRB).

Solar Radio burst (SRB) is a radio frequency emission from the Sun which starts simultaneously with the burst of EUV and X-rays that is the key feature of a solar flare. When the solar radio burst occurs, it usually starts by emitting radio waves at GHz frequencies around the time of the flare, but may continue long after the flare but with the emission frequencies gradually declining to MHz frequencies. As with solar flares these radio bursts have their origin in solar active regions. Whilst a SWF mainly affects the utility of the HF frequency range, an SRB can affect a wide range of various radio systems, such as GNSS (Sato et al., 2019b, 2019a), line-of-sight radio-communications where

the Sun lies in the collecting area of the receiver like base stations of cellular/mobile phone networks (or its side/grating lobes) (Cannon et al., 2013), and radars (Marqué et al., 2018). Whilst there has been speculation that SRBs could interfere with signal reception by cellular phone handsets, there appear to be no substantive reports of such interference, despite more than two decades of extensive global use of such handsets (Gary and Bastian, 2021).

#### (3) Polar cap absorption.

Polar Cap Absorption (PCA) is a phenomenon in which the ionisation of the D region of the ionosphere in the polar cap region is rapidly enhanced by Solar Energetic Particles (SEP) emitted by the shock waves ahead of fast coronal mass ejections (CME) and by solar flares, resulting in increased absorption of radio waves and the loss of communication using the HF band (Fig. 1(b)). This phenomenon occurs 30 min to several hours after a solar flare occurs or a fast CME is launched and, in the case of a CME, may continue for several days. PCA is similar to the SWF in that radio waves are absorbed due to anomalous ionisation in the D region. Whilst the Short Wave Fade Out occurs only in the daytime, PCA occurs day and night in the polar cap region and equatorward down to approximately 60–65 deg geomagnetic latitude, and it is stronger on the dayside compared to the nightside. Therefore, it affects aeronautical radio communications with aircraft flying over polar routes, including many key air routes between Asia and North America (Jones et al., 2005).

#### (4) Aurora disturbances.

The aurora borealis (and aurora australis) is one of the most famous phenomena seen in the upper atmosphere of the polar regions. Auroras are produced when energetic charged particles (particularly electrons) are accelerated in Earth's magnetosphere and guided by magnetic field lines so that they precipitate into the atmosphere. Here,

they excite neutral species to emit light (e.g. the striking green and red emissions from oxygen atoms) and also create ionisation, producing significant fluctuations in the electron density of the ionosphere (mainly around 100 km altitude, corresponding to the E region of the ionosphere). This electron density enhancement induced by particle precipitation in the auroral region also increases D-region absorption (e.g. Hargreaves, 1969). In addition, the presence of widespread energetic particle precipitation in the auroral and polar ionospheres can cause electron density irregularities to form over an extended interval of altitudes, thus leading to phase fluctuations of GNSS radio signals. These phase fluctuations then initiate a degradation of the positioning quality (i.e., a general increase in the positioning error accompanied by data gaps) (Hosokawa et al., 2014; John et al., 2021b; Forte et al., in press). This depends upon the gradient in electron density originated through particle precipitation and the interval of altitudes over which this gradient occurs (John et al., 2021a). For example, when ionisation associated with auroras is localised in the ionospheric E region, the gradient in electron density variations can be smaller than in the polar F region ionosphere. Examples of observations showing ionospheric phenomena other than auroras found in the polar ionosphere F region are illustrated hereafter.

#### (5) Ionospheric positive/negative storm.

Magnetic storms can cause disturbances in the diurnal variation of plasma density, which are called ionospheric storms. Ionospheric storms can be divided into ionospheric positive phase storms (positive storms), in which the plasma density increases significantly, and ionospheric negative phase storms (negative storms), in which it decreases significantly. Ionospheric positive-phase storms are caused by an increase in thermospheric winds due to heating of the polar thermosphere caused by magnetic storms, and by an eastward electric field applied from the magnetosphere to the polar regions and penetrating to low latitudes, both effects pushing ions and electrons in the ionosphere up to high altitudes. Ionospheric negative-phase storms occur when changes in atmospheric composition associated with heating of the polar thermosphere spread globally and reduce the ionospheric plasma density through enhanced dissociative recombination. This reduction is most prominent at night and will partially recover in daytime when solar EUV restores some of the missing ionisation. When an ionospheric positive-phase storm occurs, HF radio waves that normally pass through the ionosphere are reflected in the ionosphere, expanding the frequency band available for out-of-sight HF communications, so there is no effect in terms of interference. On the other hand, when an ionospheric negative phase storm occurs, HF radio waves that are normally reflected in the F region are not reflected and pass through the ionosphere, making it difficult to receive out-of-sight HF communications, especially at night (Fig. 1(c)). The frequency band of HF radio waves that are affected is the same as that of the SWF, but the difference is that the SWF is caused by solar flares and lasts

from several minutes to several hours, whereas negative phase storms in the ionosphere are caused by magnetic storms and last from several hours to several days, with some gradual recovery during daytime hours.

#### (6) Travelling Ionospheric Disturbances (TID).

Travelling Ionospheric Disturbance (TID) is a well-known phenomenon in which fluctuations in ionospheric electron density are generated by atmospheric gravity waves (AGW) and propagate with those AGWs. They have been observed and studied extensively (Hunsucker, 1982; Hocke and Schlegel, 1996). Based on their characteristics, TIDs are classified as Medium-Scale TIDs (MSTIDs) with periods of 15–60 min and horizontal wavelengths of a few hundred kilometres, and Large-Scale TIDs (LSTIDs) with periods of 30 min to 3 h and horizontal wavelengths of 1000 km or more. LSTIDs are caused by atmospheric gravity waves generated at high latitudes by geomagnetic disturbances and propagate equatorward. Other sources of gravity waves that can produce TIDs include a range of lower atmosphere/surface phenomena such as convective clouds/thunderstorms (Chowdhury et al., 2023), tsunamis (Chou et al., 2020), and explosions both natural (Themens et al., 2022) and human-made (Jonah et al., 2021). However, TIDs can be a source of residual errors in relative positioning such as in real-time kinematic or differential GNSS. Single-point precise positioning offers a possible solution to this problem: however, when performed in real-time, precise single-point positioning relies upon correction services based on the modelling of errors over wide areas. In this case, TIDs may still introduce residual errors. TIDs also have a significant impact on scientific observations made by arrays of radio telescopes: although there exist to calibrate radio astronomy observations (Pearson and Readhead, 1984), ionospheric effects still represent a challenge for future frontiers (e.g., the epoch of reionisation) and infrastructure (e.g., the Square Kilometre Array Observatory). Examples of propagation effects on radio waves received from radio objects and induced by ionospheric structures associated with TIDs are contained in works such as Fallows et al. (2020), Fallows et al. (2016). Recent studies (Belehaki et al., 2020) have explored techniques for routine detection of TIDs and have led to the deployment of the TechTIDE service reporting TID detections over Europe (<https://techtide.space.noa.gr/>).

#### (7) EPBs.

A plasma bubble is a phenomenon in which a region of locally low electron density develops like a “bubble” after local sunset in the ionosphere at low latitudes near the magnetic equator (Fig. 2). The plasma bubbles form across the magnetic equator and tend to drift eastward. When solar activity is high or when a magnetic storm occurs, bubbles can form over a wider geographical area thus reaching mid-latitude regions such as Japan. As a result, radio links at lower elevation angles equatorward of those regions may experience disturbances associated with the intersection of irregularities within extended EPBs. Spatial variations in electron density inside and around plasma bubbles are



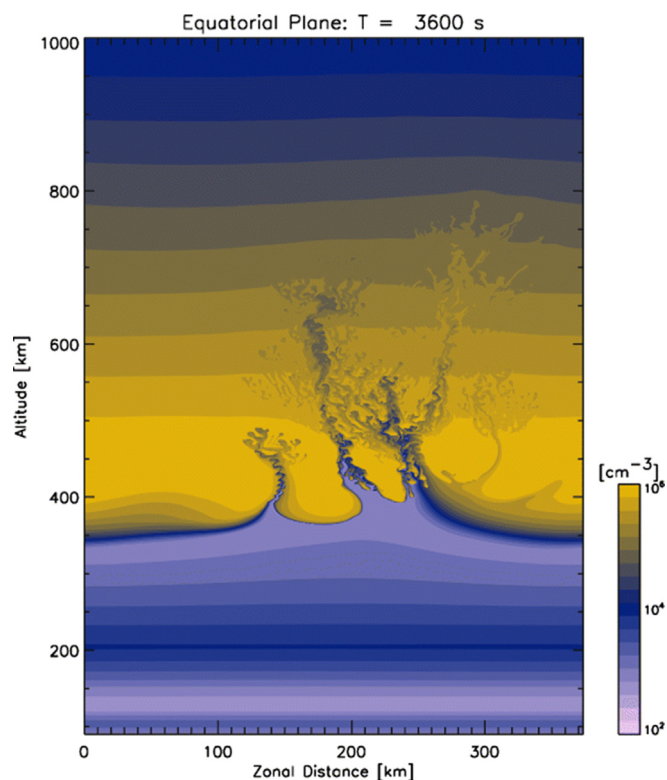


Fig. 2. Numerical simulation results of Equatorial Plasma Bubbles (Yokoyama, 2017).

large and affect the propagation of radio waves in the HF to L bands. In the HF band, changes in the direction of radio propagation due to the substructure of the plasma bubble and anomalous propagation along the plasma bubble structure are possible, but they have little impact in terms of interference in HF communications.

Radio waves used in satellite communications and navigation usually pass through the ionosphere, but irregular plasma structures associated with plasma bubbles and other phenomena can cause short-period fluctuations in signal reception strength. This is the phenomenon of “ionospheric scintillation” as previously noted above, which can lead to degradation of the signal quality, leading to loss of data if the signal protocol does not mitigate for such degradation (Vani et al., 2019). It can also lead to disturbances in images recorded by satellite-based synthetic aperture radars. This equatorial manifestation of scintillation has been known for a long time, and it is known to affect satellite communications such as Inmarsat in Japan (Karasawa et al., 1985). In March 2002, during the U.S. military’s “Anaconda” operation, UHF satellite communications (SATCOM) were disrupted, resulting in human casualties on the U.S. military side. EPB was pointed as a possibility of the cause of the disruption of communication (Kelly et al., 2014).

Scintillation due to the ionosphere has a smaller effect at higher frequencies, and in satellite communication systems above 10 GHz, it is almost negligible compared to other

effects such as tropospheric scintillation and rain fade. On the other hand, in the case of satellite communication systems utilising radio waves with carrier frequencies in VHF, UHF, L-band (1–2 GHz band) and S-band (2–4 GHz band), the effect of scintillation caused by ionospheric plasma bubbles is prevalent. In general, the longer the radio propagation path through the plasma bubble structure (for example, extending north–south along the magnetic field lines), the greater the effect.

#### (8) Es layer.

The Es layer is a dense layer of metal ions that forms in conjunction with wind shears around 110 km, gradually descending to about 100 km (Haldoupis, 2011), and eventually decaying by recombination. These so-called sporadic-E layers tend to occur frequently in summer (Taguchi and Shibata, 1961) and, at that time, may appear as a series of events, each exhibiting a descent as noted above. When the direction of propagation of radio waves into the ionosphere becomes oblique and the angle of incidence increases, the reflective frequency increases. This can cause interference with distant communications outside the line of sight (Fig. 1(d)).

Fig. 3 shows a schematic of the effects of the Es layer on air navigation: the Es layer allows VHF radio waves (108–137 MHz for commercial aviation) emitted from out-of-sight ground stations to reach aircraft, causing interference. Monitoring observations of VHF air navigation message propagation in Kure City, Hiroshima Prefecture, Japan, have received radio waves from numerous out-of-sight transmitting points (Sakai et al., 2019).

#### (9) Polar patches.

Polar patches are clouds of enhanced F-region ionisation that drift across the polar ionosphere from the dayside to the nightside. They have scale sizes of 100 s of kilometres and electron densities at least twice that of the surrounding ionosphere (Wood et al., 2009). Polar patches are thought to be an ionospheric response to magnetic reconnection on the dayside magnetopause. Momentum from the solar wind enters the magnetosphere via magnetic reconnection (Dungey, 1961) and drives a flow of plasma across the polar ionosphere from the dayside to the nightside (Axford and Hines, 1961). The bursty nature of reconnection can vary the rate at which plasma, generated on the dayside by solar EUV, enters the cross-polar flow, thus breaking up that flow into clouds of denser plasma that we observe as polar patches. The lifetime of F-region plasma is usually several hours, so these patches can persist as they travel over to the nightside. Polar patches have significant impacts on the use of *trans*-ionospheric radio links in polar regions, particularly in the Arctic because of the growing range of commercial activities in that region, e.g. air and shipping routes, tourism, mineral and hydrocarbon exploitation. For example, as noted above, high-frequency radio is a critical technology for communications with aircraft crossing the Arctic, so it is important to assess the impact of polar patches on such communications (Warrington et al., 2016; Thayaparan et al., 2021).

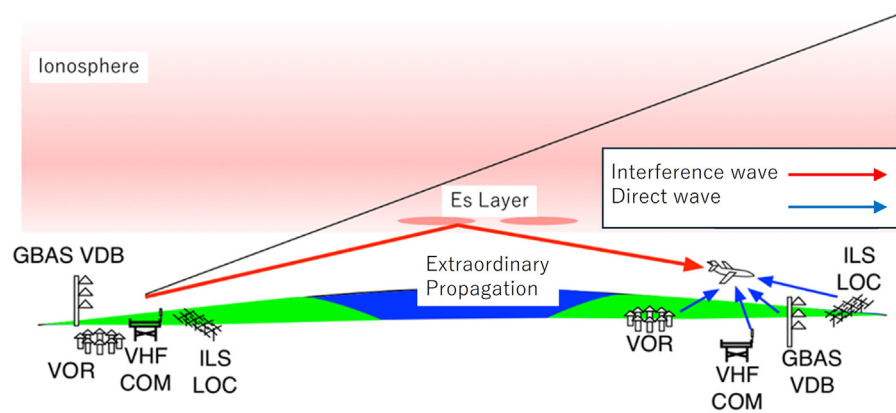


Fig. 3. A schematic plot of the effects of an Es layer on radio waves used in aeronautical navigation (Sakai et al., 2019). The black, blue and red arrow show the radio propagation from the VOR, interference wave by Es-Layer and direct wave from the nearest station.

Polar patches also contain electron density irregularities capable of disturbing GNSS radio signals at L band. Due to the combination between the field-aligned nature of the irregularities and the ray path geometry for typical GNSS links, these irregularities mainly induce phase fluctuations and data outages which can severely degrade the positioning quality and the availability of safety-critical services (e.g. in civil aviation) (John et al., 2021a, 2021b). The disruption induced by polar patches (as well as that induced by particle precipitation) intensifies in the presence of disturbed magnetic conditions (Forte et al., in press), hence degrading the positioning quality and limiting the availability of augmentation systems.

The propagation disturbances induced by irregularities associated with polar patches and with particle precipitation are expected to be more prominent on L-band radio signals from LEO constellations (such as those that may be utilised for positioning in the future): a higher ray path elevation in these cases would imply propagation through more irregularities structure and, hence, the likelihood for higher intensity scintillation (Fremouw et al., 1978) that can enhance the occurrence of data outages. Therefore, the impact of disturbances associated with both polar patches and particle precipitation in the high-latitude ionosphere will need proper consideration in the future.

### 3. Discussion

The phenomena explained in the previous section are summarised in Table 1.

To mitigate these impacts on communication and navigation, we need to address the lead time between forecast and occurrence time. We can categorise these phenomena in three groups with their sources; (1) SWF and SRB, (2) SEP and PCA, (3) CMEs driving storms, aurora, TIDs and polar patches, and (4) not triggered by solar flare and CMEs (EPB, Es). These categories are based on the time between the occurrence of flare and the occurrence of the phenomena at Earth. In Category 1, SWF and SRB occur simultaneously when the electromagnetic radiation associ-

ated with the flare arrives at the Earth, and Category 2 occurs around 30 min after that. Category 3 occurs 1 to 3 days after the occurrence of source flare and eruption. Category 4 occurs independently from solar flares and CMEs.

The occurrence time of category 1 is close to that of solar flare, so it is critical to improve solar flare forecasts for extending the lead time. Recent activities show work using artificial intelligence for predicting solar flares, (e.g., Nishizuka et al., 2017; Georgoulis et al., 2021), and also using numerical models e.g., Kusano et al., 2020. These studies have potential to extend the lead time for preparedness. Looking ahead it is important to consider whether the most promising routes for flare forecasting are statistical, rather than deterministic (because of the nature of the reconnection process that drives flares), and hence what that implies for forecasting of category 1 phenomena. It will be important to discuss with forecast users on how they might make use of statistical forecasts of category 2. This type of feedback (operations-to-research) can be helpful in guiding research towards results of practical value (Hapgood, 2022).

For category 3, there are already several models for predicting ionospheric storms, however, higher precision is required for operational use. In particular, it is important to consider that the arrival of a CME is effectively a shock input to the ionosphere - in the sense that the ionosphere contains no information on the approaching CME. Thus, prior forecasting of ionospheric storms must be based on insights into conditions in the solar wind upstream of Earth, together with initial conditions measured in the ionosphere. As has long been noted, forecasts based on internal properties of the ionosphere are generally useful only with lead times of minutes. Recent work by Tsagouri and Belehaki, 2022 is a good example of the need for forecasts based on upstream solar wind conditions. They report the results of the recent validation tests on the performance of the Solar Wind driven autoregression model for ionospheric forecast (SWIF), which is driven by interplanetary magnetic field data taken near the Lagrange L1 point, a key location for monitoring the

Table 1  
Ionospheric phenomena, area, duration and utilities which affect radio communication, GNSS, and satellite communications.

Phenomena	Affecting area	Affecting duration	Affected Ionospheric region	Affecting utilities
Short Wave Blackout from solar flare	Dayside of the Earth, maximum around equator region	Several min – several hours	D region	HF, VHF, LF, VLF
Short Wave Blackout from REP events	Mid latitudes	Several min - several hours	D region	HF, LF, VLF
Solar Radio Burst	Dayside of the Earth, maximum around equator region	Several min – several hours	–	Various
Polar Cap Absorption	High Latitude Region	Several min – several days	D region	HF
Auroral disturbances	Auroral Oval	Several hours	D and E region	HF, GNSS
Ionospheric positive storm	Global	Several hours	F region	GNSS
Ionospheric negative storm	Global	Several hours	F region	HF
TIDs	Global	Several hours	F region	GNSS, VHF
EPBs	Local post-sunset and nighttime of equatorial and mid-latitude region	Several hours after local sunset	F region	GNSS
Es layer	Dayside of the Earth	Several min - hours	Es	HF, VHF
Polar patches	Polar regions	Several hours	F region	HF, GNSS, satcom

upstream solar wind. These trials will improve the precision of ionospheric forecasts in the future. Further trials should be encouraged using both physics-based and machine-learning approaches to forecasting. In addition, it is also important to estimate when the CME arrives to the Earth to prepare to mitigate the impact. [Fallows et al. \(2022\)](#) shows a new trial of Interplanetary Scintillation visualisation which helps to estimate the velocity of CME and its arrival time.

In addition, it is important to mention that ionospheric storm can occur in response to a sudden southward turning in the IMF not related to a CME, or to Coronal Holes or HSS.

For category 4, it is difficult to find any precursors of Es and EPB, so it is important to build observation networks for monitoring these ionospheric disturbances globally, e.g., satellite constellations and data sharing of ground-based observation. For example, [Tsagouri et al., 2023a](#) reports recent activities of ground and space-based ionospheric observation. In addition, they discuss the data quality and accuracy which is important for global ionospheric monitoring systems. These efforts will contribute to improving the activities in category 4.

For all four categories, it is important to recognise that, as discussed in [Tsagouri et al., \(2023b\)](#), the prediction and forecast of the ionosphere is still challenging because the physics of the thermosphere-ionosphere system is still not fully understood. It is also important to understand how operators of systems vulnerable to space weather can make best use of space weather forecasts and to focus the development of forecasting towards their needs, not just what seems best science. This approach to forecast development is part of the virtuous circle, Research to Operation and Operation to Research (R2O2R), advocated by [Opgenoorth et al \(2019\)](#) and [Hapgood \(2022\)](#) in which space weather research feeds into operations, but operations then feed back insights and ideas into research. An example of this activity could be also found in [Cesaroni et al. \(2020\)](#) where a novel empirical model was introduced to forecast, 24 h in advance, the Total Electron Content (TEC) on a global scale.

Another key element in R2O2R is that the space weather impact, not only for communication and navigation but also for other critical infrastructure, depends on the technical specifications of the system. For example, in GNSS single frequency receivers are significantly more affected than multiple frequency receivers by the delay of signal propagation in the ionosphere. The better resilience of multiple frequency receivers arises from their ability to cancel the first-order ionospheric delay more effectively (by using different frequencies to remove the ionospheric delay). In most cases, to assess the space weather impact on critical infrastructures, it is necessary to know the details of the system, and its operating concepts and procedures, and to have dialogue with engineering communities.

An area where R2O2R is particularly important and will be increasingly more relevant is represented by applications



reliant upon GNSS. Here, challenges associated with the physics of ionospheric irregularities, their propagation disturbances at L band, and the specifications of the various systems combine in a multi-layered problem.

In the case of GNSS applications, various mitigation strategies are attempted although none of these is capable of completely and effectively removing the vulnerability to the degradation suffered by GNSS under adverse space weather conditions. In general, the mitigation strategies of relevance to GNSS applications have been developing in essentially three areas: (1) user-level, (2) system-level, and (3) forecasts.

#### 1. User-level mitigation strategies

These types of mitigation strategies include modifications to settings in the receiver (e.g., pre-detection bandwidth, tracking loops bandwidths) in an effort to increase the capability of a receiver to maintain lock in the presence of enhanced intensity scintillation (at equatorial latitudes) or phase fluctuations (at high latitudes). These approaches offer limited advantages because of the complexity in the optimisation of the tracking problem. This limitation has led to the adoption of various strategies aimed at the improvement of positioning algorithms (both in real-time and in post-processing) that aim, for example, at modelling the errors for those satellites more exposed to scintillation and phase fluctuations. These approaches also show relatively limited advantages due to the complexity and non-stationary nature of the errors in the observables. Recently, an approach based on the estimate of the positioning solution over shorter time intervals (e.g., shorter than 30 s) has shown potential towards the improvement of the positioning quality both at equatorial and high latitudes (Vani et al., 2019; John et al., 2021b); however, this approach remains sensitive to the duration of data gaps.

Along the line of user-level mitigation strategies are the Receiver Autonomous Integrity Monitoring (RAIM, aimed at GPS) and the Advanced Receiver Autonomous Integrity Monitoring (ARAIM, aimed at other GNSS constellations). These techniques are utilised to detect faults and threats to the integrity of the GPS (RAIM) or GNSS (ARAIM) solution by evaluating the consistency between the measurements from available satellites.

#### 2. System-level mitigation strategies

This type of mitigation strategies offers additional corrections that can reduce ionospheric residual errors in the positioning solution. Examples of system-level mitigation strategies include Satellite-Based Augmentation Systems (SBAS) addressed to civil aviation (such as EGNOS, WAAS, GAGAN), regional systems (e.g., NavIC in India, QZSS in Japan), Ground-Based Augmentation Systems (GBAS, typically deployed at airports), network corrections for PPP. These approaches are in support of sectors such as civil aviation (Kauristie et al., 2021), and their limitation lies in the necessity of some sort of spatial averaging to estimate corrections over a large area, which results in the loss of sensitivity to smaller scale effects (e.g., scintillation).

#### 3. Forecasts

There are growing efforts in the attempt to forecast the occurrence of propagation disturbances such as scintillation and phase fluctuations. These efforts are based on the use of physical models, their augmentation through data ingestion/assimilation, and recently the use of machine learning. Important challenges in these efforts include the modelling of drivers responsible for day-to-day variability in the ionosphere and the sparsity in experimental data. These challenges reduce the sensitivity to smaller scale irregularities and the capability to produce accurate forecasts, hence suggesting the need for more systematic, integrated, and comprehensive monitoring systems. An additional challenge is represented by the need to translate typical indices that quantify ionospheric propagation disturbances in an impact (or risk) for users (Forte et al., in press; Forte and Radicella, 2005), thus suggesting the need to integrate typical ionospheric observations with real impact for users, as discussed in Forte et al. (in press).

Another example of feedback in this topic area is that the nowcasting of category 1 phenomena and their impacts on radio systems can be aided by monitoring flare effects, as noted previously, on the VLF signals (3 – 30 kHz) commonly transmitted for communication with submarines and other purposes. The operational Global Ionosphere Flare Detection System (GIFDS), developed for flare monitoring and detection, has great potential to warn users in case of extreme flares with a delay of less than 1 min (Wenzel et al., 2016). The measurements are based on recording signal modifications due to flare-induced changes in the lower ionosphere. The timely information on strength and expected dynamics of solar flare activity is needed to ensure reliable terrestrial High Frequency (HF) communication because these events induce enhanced signal absorption in the ionosphere up to black out. In combination with GNSS measurements (TEC gradients) it is possible to directly identify the impact of a flare on the different user domains, for example, in communication and navigation, which strongly depends on the flare spectrum. A strong X-ray component has an impact on communication, whereas a strong EUV component can cause ionospheric gradients and disturbances in navigation.

#### 4. Summary and recommendation

As we have outlined above, there are several types of space weather phenomena that affect radio communication and navigation. There has been much recent progress in mitigating these impacts, e.g. through the deployment of technologies that monitor the integrity of GNSS signals against space-weather driven changes in TEC. These include augmentation systems such as WAAS in the US, EGNOS in Europe, regional systems such as GAGAN (and, more recently, NavIC) in India, MSAS (and, more recently, QZSS) in Japan, and also technologies such as receiver autonomous integrity monitoring (RAIM) that is now widely used, for example, in maritime navigation.



Nonetheless, there is still much to do to mitigate other space weather impacts on radio systems, as we have noted above. For this reason, we recommend a number of actions to improve our ability to forecast and monitor space weather effects in the ionosphere. These actions should not only address ionospheric science, but also important issues from other domains including (a) the solar, heliospheric, magnetospheric and thermospheric drivers of ionospheric phenomena, and (b) an understanding of how operators of vulnerable systems can use forecasts and thus provide insights into how forecasts can deliver truly actionable information. In that over-arching context, we recommend implementing the following actions.

Action 1: Improving the precision of solar flare, SRB and SEP forecasts, exploring what is feasible in a context of statistical forecasting and how this may be of value to operators of vulnerable systems.

Action 2: Improving the precision of ionospheric storm forecast, exploring how we can use measurements and forecasts of upstream solar wind conditions to drive forecasts, and, as with solar flares, how ionospheric forecasts may be of value to operators (for example, by translating ionospheric observations into impact that operators need to manage).

Action 3: Building and maintaining global and real time ionospheric monitoring systems including constellation satellites and ground-based measurements.

Action 4: Securing long-term preservation of ionospheric data for future studies of space weather impacts. Long-term datasets are key resources for the development and validation of forecast models.

Action 5: Strengthening links with other scientific communities affected by space weather effects in the ionosphere (for example, Earth Observation, geodesy, radio astronomy) and with users (for example, in sectors such as civil aviation, maritime transport, time synchronisation, space exploration, in-orbit operations, autonomous navigation) in order to allow effective R2O2R.

## Declaration of competing interest

The authors declare the following financial interests/personal relationships which may be considered as potential competing interests: Mamoru Ishii reports financial support, administrative support, article publishing charges, and travel were provided by National Institute of Information and Communications Technology.

## Acknowledgements

The work carried out by BF at the University of Bath was supported by the UK Natural Environment Research Council [Grant number NE/R009082/1, Grant number NE/V002597/1, and Grant number NE/W003074/1].

Fig. 2 is provided from Yokoyama (2017) originally published by Springer.

## References

- Axford, W.I., Hines, C.O., 1961. A unifying theory of high-latitude geophysical phenomena and geomagnetic storms. *Canadian J. Phys.* 39 (10), 1433–1464. <https://doi.org/10.1139/p61-172>.
- Belehaki, A., Tsagouri, I., Altadill, D., Blanch, E., Borries, C., Buresova, D., Watermann, J., 2020. An overview of methodologies for real-time detection, characterisation and tracking of traveling ionospheric disturbances developed in the TechTIDE project. *J. Space Weather Space Clim.* 10, 42. <https://doi.org/10.1051/swsc/2020043>.
- Berdermann, J., Sato, H., Kriegel, T.M., Fujiwara, T., Tsujii, T., 2020. Effects Of Equatorial Ionospheric Scintillation For GNSS Based Positioning In Aviation. In: 2020 European Navigation Conference (ENC), Dresden, Germany, pp. 1–8. <https://doi.org/10.23919/ENC48637.2020.9317407>.
- Berdermann, J., Kriegel, M., Banys, D., Heymann, F., Hoque, M.M., Wilken, V., Borries, C., Heßelbarth, A., Jakowski, N., 2018. Ionospheric response to the X9.3 flare on 6 September 2017 and its implication for navigation services over Europe. *Space Weather* 16 (10), 1604–1615. <https://doi.org/10.1029/2018SW001933>.
- Cannon, P., Angling, M., Barclay, L., Curry, C., Dyer, C., Edwards, R., Underwood, C., 2013. Extreme space weather: impacts on engineered systems and infrastructure. *Royal Acad. Eng.* [https://raeng.org.uk/media/1z2fs5ql/space\\_weather\\_full\\_report\\_final.pdf](https://raeng.org.uk/media/1z2fs5ql/space_weather_full_report_final.pdf).
- Cesaroni, C., Spogli, L., Aragon-Angel, A., Fiocca, M., Dear, V., De Franceschi, G., Romano, V., 2020. Neural network based model for global total electron content forecasting. *J. Space Weather Space Clim.* 10, 11. <https://doi.org/10.1051/swsc/2020013>.
- Cesaroni, C., Spogli, L., Franceschi, G.D., Damasceno, J.G., Grzesiak, M., Vani, B., Monico, J.F.G., Romano, V., Alfonsi, L., Cafaro, M., 2021. A measure of ionospheric irregularities: zonal velocity and its implications for L-band scintillation at low-latitudes. *Earth Planet. Phys.* 5 (5), 450–461. <https://doi.org/10.26464/epp2021042>.
- Chou, M.-Y., Cherniak, I., Lin, C.C.H., Pedatella, N.M., 2020. The persistent ionospheric responses over Japan after the impact of the 2011 Tohoku earthquake. *Space Weather* 18. <https://doi.org/10.1029/2019SW002302> e2019SW002302.
- Chowdhury, S., Kundu, S., Ghosh, S., Sasmal, S., Brundell, J., Chakrabarti, S.K., 2023. Statistical study of global lightning activity and thunderstorm-induced gravity waves in the ionosphere using WWLLN and GNSS-TEC. *J. Geophys. Res.: Space Phys.* 128. <https://doi.org/10.1029/2022JA030516> e2022JA030516.
- Dellinger, J.H., 1937. Sudden ionospheric disturbances. *Terr. Magn. Atmos. Electr.* 42 (1), 49–53. <https://doi.org/10.1029/TE042i001p00049>.
- Demirkol, M.K., Inan, U.S., Bell, T.F., Kanekal, S.G., Wilkinson, D.C., 1999. Ionospheric effects of relativistic electron enhancement events. *Geophys. Res. Lett.* 26 (23), 3557–3560. <https://doi.org/10.1029/1999GL010686>.
- Dungey, J.W., 1961. Interplanetary magnetic field and the auroral zones. *Phys. Rev. Lett.* 6 (2), 47. <https://doi.org/10.1103/PhysRevLett.6.47>.
- Fallows, R., Bisi, M.M., Forte, B., Ulich, T., Konovalenko, A.A., Mann, G., Vocks, C., 2016. Separating nightside interplanetary and ionospheric scintillation with lofar. *Astrophys. J. Lett.* 828. <https://doi.org/10.3847/2041-8205/828/1/L7>.
- Fallows, R., Forte, B., Astin, I., Allbrook, T., Arnold, A., Wood, A., Dorrian, G., Mevius, M., Rothkaehl, H., Matyjasiak, B., Krankowski, A., Anderson, J.M., Asgekar, A., Avruch, I.M., Bentum, M.J., Bisi, M.M., Butcher, H.R., Ciardi, B., Dabrowski, B., Damstra, S., de Gasperin, F., Dusch, S., Eisloffel, J., Franzen, T.M.O., Garrett, M. A., Griebmeier, J.-M., Gunst, A.W., Hoeft, M., Horandel, J.R., Iacobelli, M., Intema, H.T., Koopmans, L.V.E., Maat, P., Mann, G., Nelles, A., Paas, H., Pandey, V.N., Reich, W., Rowlinson, A., Ruiter, M., Schwarz, D.J., Serylak, M., Shulevski, A., Smirnov, O.M., Soida, M., Steinmetz, M., Thoudam, S., Toribio, M.C., van Ardenne, A., van Bommel, I.M., van der Wiel, M.H.D., van Haarlem, M.P., Vermeulen, R.C., Vocks, C., Wijers, R.A.M.J., Wucknitz, O., Zarka, P., Zucca, P.,

2020. A LOFAR observation of ionospheric scintillation from two simultaneous travelling ionospheric disturbances. *J. Space Weather Space Clim.* 10 (10), 1–16. <https://doi.org/10.1051/swsc/2020010>.
- Fallows, R.A., Iwai, K., Jackson, B.V., Zhang, P., Bisi, M.M., Zucca, P., 2022. Application of novel interplanetary scintillation visualisations using LOFAR: A case study of merged CMEs from september 2017. *Adv. Space Res.* <https://doi.org/10.1016/j.asr.2022.08.076>.
- Forte, B., Bastian, T.S., 2021. Solar radio burst effects on radio- and radar-based systems. In: Coster, A.J., Erickson, P.J., Lanzerotti, L.J., Zhang, Y., Paxton, L.J. (Eds.), *Space Weather Effects and Applications*. <https://doi.org/10.1002/9781119815570.ch6>.
- George, H.E., Rodger, C.J., Clilverd, M.A., Cresswell-Moorcock, K., Brundell, J.B., Thomson, N.R., 2019. Developing a nowcasting capability for X-class solar flares using VLF radiowave propagation changes. *Space Weather* 17, 1783–1799. <https://doi.org/10.1029/2019SW002297>.
- Georgoulis, M.K., Bloomfield, D.S., Piana, M., Massone, A.M., Soldati, M., Gallagher, P.T., Worsfold, M., 2021. The flare likelihood and region eruption forecasting (FLARECAST) project: flare forecasting in the big data & machine learning era. *J. Space Weather Space Clim.* 11 (39), 1348–1373.
- Grach, V.S., Artemyev, A.V., Demekhov, A.G., Zhang, X.-J., Bortnik, J., Angelopoulos, V., et al., 2022. Relativistic electron precipitation by EMIC waves: importance of nonlinear resonant effects. *Geophys. Res. Lett.* 49. <https://doi.org/10.1029/2022GL099994> e2022GL099994.
- Haldoupis, C., 2011. A tutorial review on sporadic E layers. *Aeronomy Earth's Atmosphere Ionosphere*, 381–394.
- Hapgood, M., 2022. Ionospheric science: An example of the importance of diversity in approaches to scientific research. *Atmos.* 13 (3), 394. <https://doi.org/10.3390/atmos13030394>.
- Hargreaves, J.K., 1969. Auroral absorption of HF radio waves in the ionosphere: a review of results from the first decade of riometry. *Proc. IEEE* 57 (8). <https://doi.org/10.1109/PROC.1969.7275>.
- Hlubek, N., Berdermann, J., Wilken, S.V., Gewies, N.S., Jakowski, M.N., Wassaie, BaylieM., Dantie, B., 2014. Scintillations of the GPS, GLONASS, and Galileo signals at equatorial latitude. *J. Space Weather Space Clim.* 4, A22. <https://doi.org/10.1051/swsc/2014020>.
- Hocke, K., Schlegel, K., 1996. A review of atmospheric gravity waves and traveling ionospheric disturbances: 1982–1995. *Ann. Geophys.* 14, 917–940.
- Hosokawa, K., Otsuka, Y., Ogawa, Y., et al., 2014. Observations of GPS scintillation during an isolated auroral substorm. *Prog. Earth Planet Sci.* 1, 16. <https://doi.org/10.1186/2197-4284-1-16>.
- Hunsucker, R.D., 1982. Atmospheric gravity waves generated in the high-latitude ionosphere: a review. *Rev. Geophys.* 20, 293–315. <https://doi.org/10.1029/RG020i002p00293>.
- John, H.M., Forte, B., Astin, I., Allbrook, T., Arnold, A., Vani, B.C., Häggström, I., 2021. Performance of GPS positioning in the presence of irregularities in the auroral and polar ionospheres during EISCAT UHF/ESR measurements. *Remote Sens. (Basel)* 13 (23), 4798. <https://doi.org/10.3390/rs13234798>.
- John, H.M., Forte, B., Astin, I., Allbrook, T., Arnold, A., Vani, B.C., Häggström, I., Sato, H., 2021a. An EISCAT UHF/ ESR experiment that explains how ionospheric irregularities induce GPS phase fluctuations at auroral and polar latitudes. *Radio Sci.* 56. <https://doi.org/10.1029/2020RS007236>.
- Jonah, O.F., Vergados, P., Krishnamoorthy, S., Komjathy, A., 2021. Investigating ionospheric perturbations following the 2020 Beirut explosion event. *Radio Sci.* 56. <https://doi.org/10.1029/2021RS007302> e2021RS007302.
- Jones, J.B.L., Bentley, R.D., Hunter, R., Iles, R.H.A., Taylor, G.C., Thomas, D.J., 2005. Space weather and commercial airlines. *Adv. Space Res.* 36, 2258–2267. <https://doi.org/10.1016/j.asr.2004.04.017>.
- Karasawa, Y., Yasukawa, K., Yamada, M., 1985. Ionospheric scintillation measurements at 1.5 GHz in mid-latitude region. *Radio Sci.* 29, 643–651.
- Kauristie et al., 2021. Space weather services for civil aviation—challenges and solutions. *Remote Sens.* 13, 3685. <https://doi.org/10.3390/rs13183685>.
- Kelly, M.A., Comberiate, J.M., Miller, E.S., Paxton, L.J., 2014. Progress toward forecasting of space weather effects on UHF SATCOM after operation Anaconda. *Space Weather* 12, 601–611. <https://doi.org/10.1002/2014SW001081>.
- Kriegel, M., Jakowski, N., Berdermann, J., Sato, H., Merhsa, M.W., 2017. Scintillation measurements at Bahir Dar during the high solar activity phase of solar cycle 24. *Ann. Geophys.* 35, 97–106. <https://doi.org/10.5194/angeo-35-97>.
- Kusano, K., 2023. *Solar-Terrestrial Environment Prediction*. Springer <https://doi.org/10.1007/978-981-19-7765-7>.
- Kusano, K., Iju, T., Bamba, Y., Inoue, S., 2020. A physics-based method that can predict imminent large solar flares. *Science* 369 (6503), 587–591. <https://doi.org/10.1126/science.aaz2511>.
- Marqué, C., Klein, K.L., Monstein, C., Opgenoorth, H., Pulkkinen, A., Buchert, S., Thulesen, P., 2018. Solar radio emission as a disturbance of aeronautical radionavigation. *J. Space Weather Space Clim.* 8, A42. <https://doi.org/10.1051/swsc/2018029>.
- Fishing News, 1983. DECCA: More Gear Lost. Fishing News (UK) London, Arthur J Heighway Publications Ltd., issue dated 16 December 1983.
- Nishizuka, N., Sugiura, K., Kubo, Y., Den, M., Watari, S., Ishii, M., 2017. Solar flare prediction model with three machine-learning algorithms using ultraviolet brightening and vector magnetograms. *Astrophys. J.* 835, 156.
- Opgenoorth, H.J., Wimmer-Schweingruber, R.F., Belehaiki, A., Berghmans, D., Hapgood, M., Hesse, M., Temmer, M., 2019. Assessment and recommendations for a consolidated European approach to space weather—as part of a global space weather effort. *J. Space Weather Space Clim.* 9, A37. <https://doi.org/10.1051/swsc/2019033>.
- Pearson, T.J., Readhead, A.C.S., 1984. Image formation by self-calibration in radio astronomy. *Ann. Rev. Astron. Astrophys.* 22 (1), 97–130. <https://doi.org/10.1146/annurev.aa.22.090184.000525>.
- Sakai, J., Hosokawa, K., Tomizawa, I., Saito, S., 2019. A statistical study of anomalous VHF propagation due to the sporadic-E layer in the air-navigation band. *Radio Sci.* 54, 426–439.
- Sato, H., Jakowski, N., Berdermann, J., Jiricka, K., Heßelbarth, A., Banyś, D., Wilken, V., 2019a. Solar radio burst events on 6 September 2017 and its impact on GNSS signal frequencies. *Space Weather* 17, 816–826. <https://doi.org/10.1029/2019SW002198>.
- Sato, H., Jakowski, N., Berdermann, J., Jiricka, K., Heßelbarth, A., Banyś, D., Wilken, V., 2019b. Solar Radio Burst events on September 6, 2017 and its impact on GNSS signal frequencies. *Space Weather* 17 (6), 816–826. <https://doi.org/10.1029/2019SW002198>.
- Schrijver, C.J., Kauristie, K., Aylward, A.D., Denardini, C.M., Gibson, S. E., Glover, A., Vilmer, N., 2015. Understanding space weather to shield society: A global road map for 2015–2025 commissioned by COSPAR and ILWS. *Adv. Space Res.* 55 (12), 2745–2807. <https://doi.org/10.1016/j.asr.2015.03.023>.
- Taguchi, S., Shibata, H., 1961. World maps of foEs. *J. Radio Res. Lab.* 8, 355–389.
- Thayaparan, T., Warrington, E.M., Stocker, A.J., Siddle, D.R., 2021. Simulation of the effect of convecting patches of enhanced electron density on HF over-the-horizon radars (OTHRs) in the polar regions. *IEEE Geosci. Remote Sens. Lett.* 18 (9), 1570–1574. <https://doi.org/10.1109/LGRS.2020.3045926>.

- Themens, D.R., Watson, C., Žagar, N., Vasylyevych, S., Elvidge, S., McCaffrey, A., et al., 2022. Global propagation of ionospheric disturbances associated with the 2022 Tonga volcanic eruption. *Geophys. Res. Lett.* 49. <https://doi.org/10.1029/2022GL098158>.
- Tsagouri, I., Belehaki, A., 2022. Assessment of solar wind driven ionospheric storm forecasts: The case of the solar wind driven autoregression model for ionospheric forecast (SWIF). *Adv. Space Res.* <https://doi.org/10.1016/j.asr.2022.06.047>.
- Tsagouri, I., Belehaki, A., Themens, D.R., Jakowski, N., Fuller-Rowell, T., Hoque, M.M., Grzegorz Nykiel, W., Miloch, J., Borries, C., Morozova, A., Barata, T., Engelke, W., Shim, J., 2023a. Ionosphere Variability I: Advances in observational, monitoring and detection capabilities.
- Tsagouri, I., Themens, D.R., Belehaki, A., Shim, J., Hoque, M.M., Nykiel, G., Borries, C., Morozova, A., Barata, T., Miloch, W.J., 2023. Ionospheric variability II: advances in theory and modeling. *Adv. Space Res.* <https://doi.org/10.1016/j.asr.2023.07.056>.
- United States Coast Guard, 1992. “Skywave Delay” in Loran-C User Handbook. P. 133, <https://media.defense.gov/2021/Oct/26/2002879902/-1/-1/0/LORANCUSERSHANDBOOK.PDF>
- Vani, B.C., Forte, B., Monico, J.F.G., Skone, S., Shimabukuro, M.H., Moraes, A.O., Portella, I.P., Marques, H.A., 2019. A novel approach to improve GNSS precise point positioning during strong ionospheric scintillation: theory and demonstration. *IEEE Trans. Veh. Technol.* 68 (5), 4391–4403. <https://doi.org/10.1109/TVT.2019.2903988>.
- Warrington, E.M., Stocker, A.J., Siddle, D.R., Hallam, J., Al-Behadili, H. A.H., Zaalov, N.Y., Honary, F., Rogers, N.C., Boteler, D.H., Danskin, D.W., 2016. Near real-time input to a propagation model for nowcasting of HF communications with aircraft on polar routes. *Radio Sci.* 51, 1048–1059. <https://doi.org/10.1002/2015RS005880>.
- Wenzel, D., Jakowski, N., Berdermann, J., Mayer, C., Valladares, C., Heber, B., 2016. Global ionospheric flare detection system (GIFDS). *JASTP* 138–139, 233–242. <https://doi.org/10.1016/j.jastp.2015.12.011>.
- Wood, A.G., Pryse, S.E., Moen, J., 2009. Modulation of nightside polar patches by substorm activity. *Ann. Geophys.* 27, 3923–3932. <https://doi.org/10.5194/angeo-27-3923-2009>.
- Yokoyama, T., 2017. A review on the numerical simulation of equatorial plasma bubbles toward scintillation evaluation and forecasting. *Prog. Earth Planet Sci.* 4, 37. <https://doi.org/10.1186/s40645-017-0153-6>.
- Zhang, K., Wan, G., Li, M., Xi, X., 2019. Skywave delay estimation in enhanced Loran based on extended invariance principle weighted Fourier transform and relaxation algorithm. *IET Radar Sonar Navig.* 13, 1344–1349. <https://doi.org/10.1049/iet-rsn.2018.5651>.
- Zhao, Z., Liu, J., Zhang, J., Xi, X., 2022. Sky-ground wave signal separation in enhanced Loran based on Levenberg–Marquart algorithm. *IET Radar Sonar Navig.* 16 (1), 1–8. <https://doi.org/10.1049/rsn2.12036>.